Franz-Keldysh effect and internal fields in ZnS crystals*

B. G. Yacobi and Y. Brada
The Racah Institute of Physics, The Hebrew University, Jerusalem, Israel
(Received 8 January 1974)

A specially constructed uv scanning microscope was used to detect built-in electric fields in faulted ZnS crystals by means of the Franz-Keldysh effect. External electric fields were applied both in the parallel and in the perpendicular direction with respect to the polar c axis. The Franz-Keldysh coefficients (FKC) and the reduced effective masses (μ^*) for the different crystalline axes were found for three crystallization forms of ZnS. In the hexagonal $2H$ the reduced effective mass, $\mu^*(\vec{E}\parallel\vec{c}) = 0.26m_0$, $\mu^*(\vec{E}\perp\vec{c}) = 0.22m_0$. For the $4H$ polytype, $\mu^*(\vec{E}\parallel\vec{c}) = 0.19m_0$, $\mu^*(\vec{E}\perp\vec{c}) = 0.17m_0$, for the cubic $3C$ $\mu^* = 0.12m_0$. The existence of opposing intrinsic electrical fields in the crystals was ascertained. Large variations occurred in the distribution of the intrinsic fields. The voltages applied along the c axis gave rise to inhomogeneous fields inside the crystal. The strength of the internal fields in faulted crystals with narrow polytypic regions (type I, type II) was found to be of the magnitude of 10^5 V/cm. These fields and their distribution are of major importance both in the anomalous photovoltaic effect and in the electroluminescence of these crystals.

INTRODUCTION

Recent electroabsorption measurements[1,2] have proved the existence of intrinsic electric fields in faulted ZnS single crystals. The nonuniform crystals used are in the form of platelets[3,4] with the c axis in their plane and consist of parallel strips of different birefringences, all perpendicular to the c axis. They often show tilt in their external faces as well.[5,6] The fields are due to charged dislocation sheets[4,7] appearing on the interface of two different structures because of the lattice-constant misfit involved[4] and because of the polar character of the c axis. A unique correlation was found between the direction of the polar c axis and the direction of both the anomalous photovoltaic effect[3] (APE) and the direction of the internal fields in the cubic portions of the faulted crystals.[1] The structural properties of the crystals determine both the photoelectric and electro-optic properties of the faulted ZnS crystals and therefore the crystals can be divided into four different classes. The classification is based on the range of values of the percentage of hexagonality (β) in the sample and it can be performed with a polarizing microscope ($\beta = 100$ for $2H$ and $\beta = 0$ for the cubic structure[8]:

(I) crystals of hexagonal ($2H$) structure with only very narrow lines of lower β; (II) crystals with a wide range of β including regions of $2H$ structure; (III) crystals containing many regions of low β, with a maximum of about $\beta = 20$; and (IV) crystals containing many regions of low β, with a maximum of about $\beta = 15$.

The measurement of the internal fields is based on the Franz-Keldysh effect[9,10] (FKE), i.e., the electric-field-induced shift of the absorption edge. Near the direct absorption edge, if no intrinsic fields are present, $\Delta\alpha$ (the change of the absorption coefficient) is positive and proportional to F^2 (F being the applied electric field). If intrinsic fields are also present, the external voltage either adds to the internal field—and then a positive $\Delta\alpha$ will be observed, or acts in opposition to the intrinsic field—and then the observed $\Delta\alpha$ may be negative. The directly measured parameter is the Franz-Keldysh coefficient (FKC).

This coefficient is described as[9]

$$\gamma = \Delta E_g/F^2 = e^2\hbar^2\sigma^2/24\,\mu^*K^2T^2, \tag{1}$$

where ΔE_g is the electric-field- (F) induced shift of the absorption edge, σ is the exponent in the absorption-coefficient formula

$$\alpha = \alpha_0 \exp\{\sigma[(h\nu - h\nu_0)/kT]\}, \tag{2}$$

and h, ν, e, k, T, and μ^* have the usual meaning.

That the absorption edge of ZnS is of an exponential type has been established previously.[11] Values of σ measured on the same crystals will be used in the computations.

EXPERIMENTAL

For the present work an ultraviolet optical scanning microscope (Fig. 1) was constructed and used to study the intrinsic electric fields in faulted ZnS crystals at room temperature.

The specimen on the microscope stage was illuminated by the concentrated light of a 500-W high-pressure Xe arc through a quartz prism monochromator (Hilger D225) (Fig. 1) with a spectral width of 8 Å. The wavelengths were chosen so as to give a large FKE in the investigated structures.[1] The scanning is done in the following manner: The enlarged (30×) image of the crystal can be either photographed or focused on an opaque screen containing a variable optical slit. The direction of the crystal is adjusted so that the c axis of the projection will be perpendicular to the length of this slit. A photomultiplier (EMI 6256S) is mounted

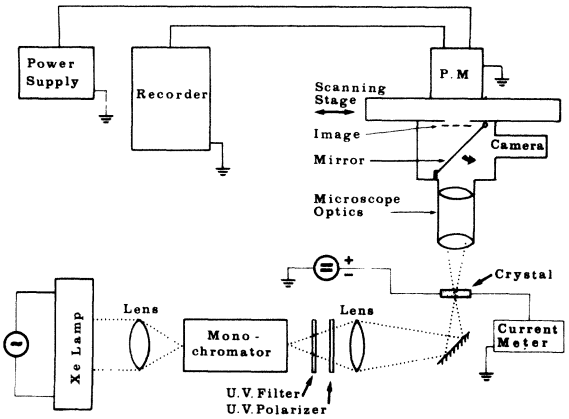

FIG. 1. Experimental setup.

above the slit and the light passing through it falls on the photocathode. The whole screen-slit-photomultiplier setup is rigidly connected on a sliding stage and moved by a stepping motor connected to a lead screw. The movement is parallel to the c axis of the projected crystal image, so that the parallel strips are scanned consecutively. Since the magnification of the optical system was about 30× and the slits on the photomultiplier were between 10 and 50 μm, even details of less than 1-μm size could be distinguished. To control the particular region to be scanned and to reduce stray light, additional slits were inserted according to need in the first focal plane of the optical system of the microscope. The crystals used in this work were platelets grown in an H_2S atmosphere at 1250 °C.[3] The crystal platelets were first observed under a polarization microscope and their thickness was also measured. Most of them were of type II or type III, the samples were mounted on an optical grade fused silica substrate. Two methods were used to apply the external electric field on the crystal. To the first samples parallel indium amalgam electrodes were applied so that the electric field was parallel to the c axis ($\vec{F} \parallel \vec{c}$). The distance between the amalgam strips ranged between 0.2 and 0.6 mm for the different specimens and this region contained many structures. The crystals were subjected to dc voltages of various magnitudes and of both polarities. The optical transmission with and without electric fields was recorded. The total sample photocurrent was measured simultaneously with a "Keithley" picoammeter. The power dissipation in the sample was kept below 0.1 mW and no electrical domain movement[12] was observed. Because of the potential barriers present in the crystal for currents along the c axis[7,13] and the inhomogeneity of the distribution of the external field, a different geometry of semitransparent gold electrodes was used in some experiments. These electrodes were evaporated on both largest surfaces of the ZnS platelets, so that the applied fields were perpendicular to the c axis ($\vec{F} \perp \vec{c}$). The distance between the electrodes varied from 7 to 50 μm according to the thickness of the different samples. The illumination in these experiments was through a Spex 1402 double monochromator with a band pass of 2 Å.

RESULTS AND DISCUSSION

Figure 2 shows the optical scan of crystal No. 296/4 (of type III) with $\vec{F} \parallel \vec{c}$ (i.e., with In-amalgam electrodes). From the observed changes in transmission of the different structures, the direction of the internal fields can be ascertained. The "positive" direction of the internal field has been designated to accord with the "positive" APE in the 3400-Å (long-wave) spectral regions, i.e., these "positive" fields would drive the current in the same direction as does the long wave APE.[1] Because of the existence of internal barriers[7,13]

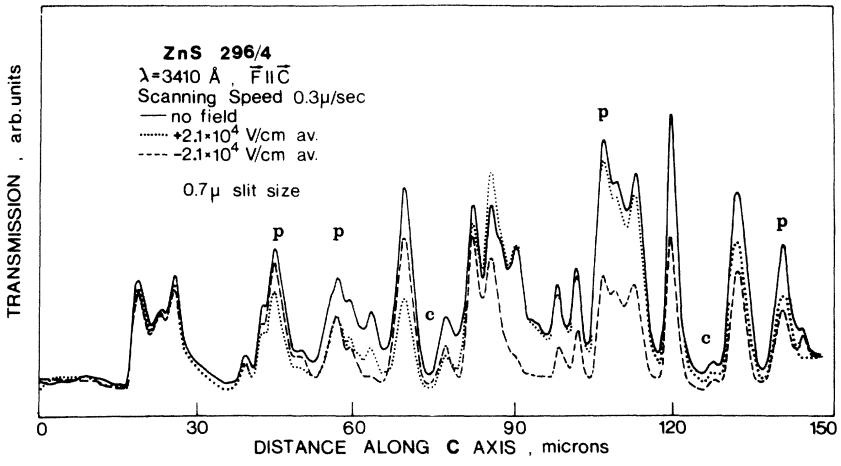

FIG. 2. Microscopic scan of crystal 296/4. Type III, In-amalgam electrodes, external field parallel to the c axis. c, cubic strips; p, polytypic strips.

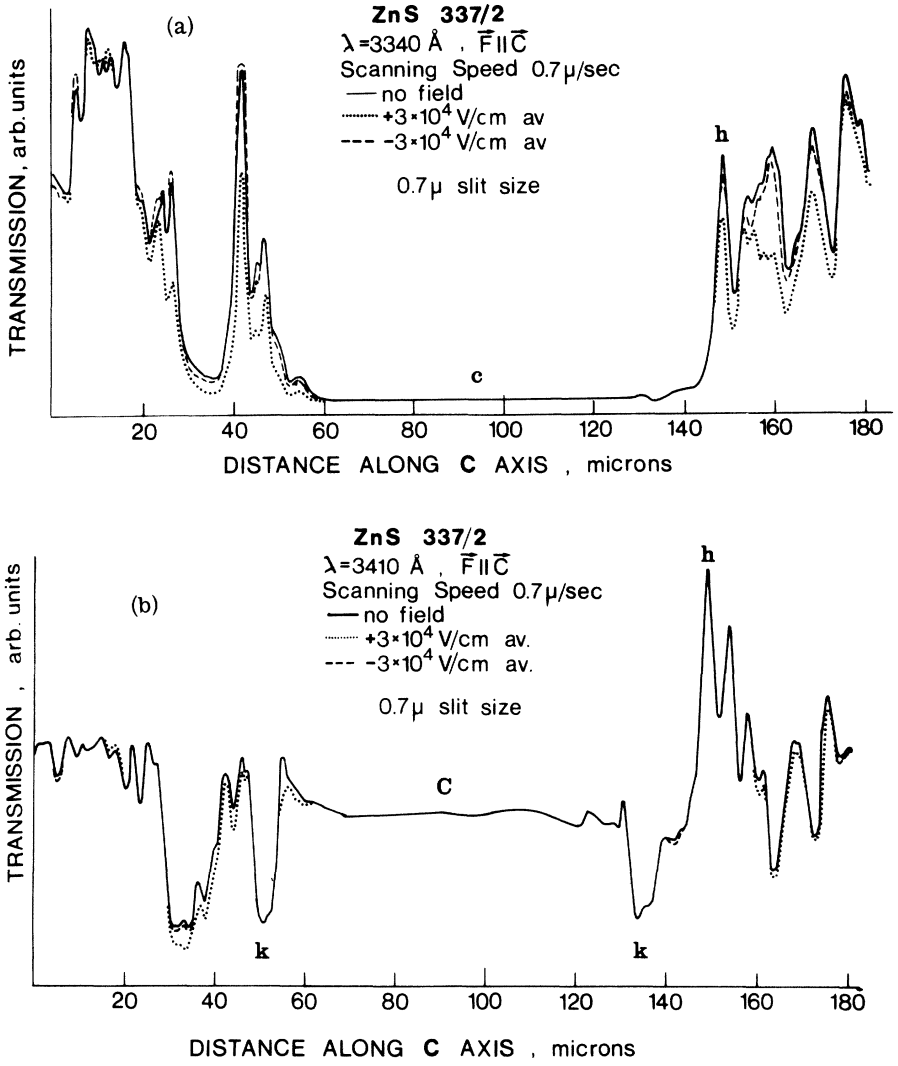

FIG. 3. Microscopic scan of crystal 337/2. Type II, In-amalgam electrodes, external field parallel to the c axis. c, cubic region; h, hexagonal strips; k, kinks in crystal.

the distribution of the applied field is highly inhomogeneous inside the crystal. This is of course accentuated by the inevitable photoconductivity appearing in all the optically absorbing structures. Judging by the observed Franz-Keldysh effect, the highest fields, both intrinsic and extrinsic, are to be found in the densely faulted regions of the crystals and not in the more uniform regions. This

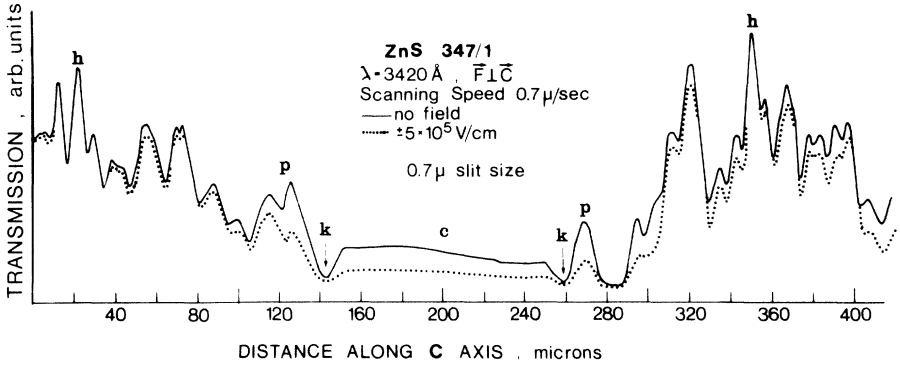

FIG. 4. Microscopic scan of crystal 347/1. Type II, evaporated semitransparent gold electrodes, external field perpendicular to the c axis. c, cubic region; h, hexagonal strips; k, kinks in crystal; p, polytypes.

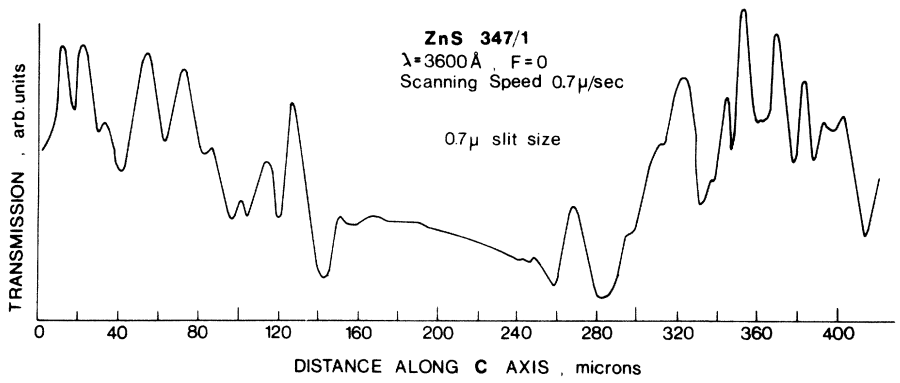

FIG. 5. Microscopic scan of crystal 347/1 at 3600 Å.

inhomogeneity of the intrinsic fields also appears on the surface in the form of changing stray fields. These inhomogeneous stray fields have been observed previously by TiO_2 particles suspended in oil.[14] The nearer the sheets of differently charged dislocations are to each other, the stronger are the expected internal fields as in wider regions a larger percentage of the field lines leave the crystal. In the wider regions there are also more photoexcited carriers available for charge compensation near the charged sheets of dislocations.[15] The magnitude of the observed transmission modulation by the external fields depends also on the wavelength of illumination.[1] Both the absorption coefficient α (Ref. 8) and the FKC depend on the percentage of hexagonality β of the structures present in the crystal studied.

The local changes of the sense of the intrinsic field which has been deduced previously in an indirect way[1] can be seen directly in Fig. 2, as in some cases the external field even increases the transmission of a structure in the crystal (negative $\Delta\alpha$) and in other cases there exists a strong asymmetry in the FKE, changing in the relative directions in different parts of the crystal.

Figure 3 refers to crystal 337/2 which is of type II and has a relatively large homogeneous cubic region in the center of the scanned portion of the crystal. Again a large FKE is observed in the highly faulted parts of the crystal. This serves as an evidence of the magnitude of both the intrinsic and extrinsic fields there, while the larger cubic region shows no FKE at all at any wavelength. There are also some constantly dark regions present, due to kink angles which will be discussed below.

Figure 4 shows the results in crystal 347/1 of type II, which is also quite similar to the previous one, but in this case the electrodes were made of evaporated semi-transparent gold with the crystal sandwiched inbetween, and the direction of the field was perpendicular to both the c axis and the width of the ZnS platelet. A clear FKE is observable in all the regions of the crystals, save in those parts (k), which because of their geometry refract the

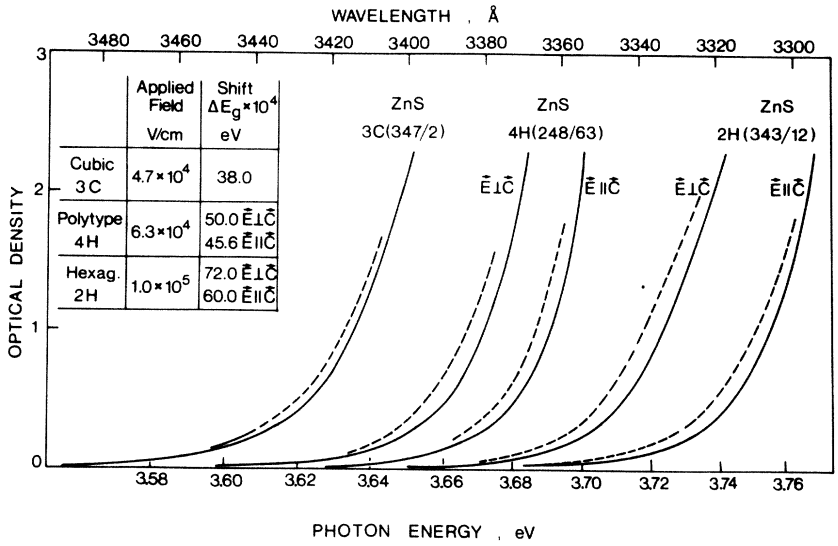

FIG. 6. Optical density of single crystals 347/2 (3C), 248/63 (4H), 343/12 (2H) at room temperature. Solid line, without electric fields; dashed line, with electric fields. Evaporated semitransparent gold electrodes, external field perpendicular to the c axis. Electrical vector of incident light both parallel ($\parallel$) and ($\perp$) to the c axis.

TABLE I. Franz-Keldysh coefficients for three crystallization forms of ZnS.

ZnS polytype	Thickness of the crystal d (μm)	Percentage of hexagonality β (%)	Franz-Keldysh coefficient $\gamma \times 10^{12}$ (eV cm^2/V^2)	Polarization of light
3C (347/2)	32	0	1.72 ± 0.05	
4H (248/63)	50	50	1.26 ± 0.04	$\vec{E} \perp \vec{c}$
			1.15 ± 0.04	$\vec{E} \parallel \vec{c}$
2H (343/12)	7	100	0.72 ± 0.06	$\vec{E} \perp \vec{c}$
			0.60 ± 0.06	$\vec{E} \parallel \vec{c}$

light away from the objective lens. These, always darker appearing regions, can be observed even with light beyond the absorption edge of the cubic ZnS, for example, at 3600 A as in Fig. 5. They are due to kink angles appearing between the surfaces of the different structures, when the crystals undergo periodic slip processes while transforming from the 2 H structure on cooling down.[5,6] In this (sandwich) case the applied and intrinsic fields are orthogonal to each other and have to be added as vectors. In relatively large homogeneous regions (> 30 μm) no significant intrinsic fields are to be detected and therefore this sandwich method was used for measuring the FKC in the 2H hexagonal structure, in the 4H polytype and in the 3C cubic structure. The results are given in Fig. 6 and Table I. From these numbers it can be seen that FKC is lowest in the hexagonal crystal, highest in the cubic crystal and intermediate in the 4H polytype.

It seems that as with other optical properties of ZnS a linear relationship exists also between the percentage of hexagonality and the FKC, but while the FKC decreases with β, both the absorption edge energy and the birefringence increase linearly with β.[8]

From these results and the σ measured in our laboratory (Fig. 6) the reduced effective mass μ^*,

$$1/\mu^* = 1/m_e^* + 1/m_h^*, \tag{3}$$

can be deduced. The results are shown in Table II. Only thin crystals remain hexagonal at room temperature. The hexagonal specimen quoted above was only about 7 μm thick and the incertainty in measuring this thickness introduced the relatively large possible errors in the results.

As can be seen from Table II, our results correspond quite well to most experimental[16] and theoretical values[17] obtained for ZnS crystals. Only one group[18] quotes quite different results for the reduced effective mass. The reduced effective mass is seen to increase approximately linearly with β. The theoretical treatment available[17] deduces the 2H structure band parameters from the 3C parameters by introducing a small hexagonal perturbing crystal field. The interaction with the extra states of the 2H structure contributes to the band parameters of the top of the valence band (Γ_9, Γ_7) specially through the interaction with the Γ_6 state. However, the band parameters at Γ_{1c} are assumed to be the same in both structures.[17] Our experimental results mean, therefore, that the effective mass of the holes is bigger in the more hexagonal structures to a greater measure

TABLE II. Reduced effective masses for three crystallization forms of ZnS.

ZnS crystal	Edge slope (present work)	μ^* (present work) in units of m_0	μ^* (Calc. Cardona (Ref. 17) in units of m_0		μ^* (Expt. Miklosz *et al.*, Ref. 16) in units of m_0	μ^* (Expt. Schanda *et al.*, Ref. 18) in units of m_0
Cubic (3C)	2.05 ± 0.10	0.12 ± 0.02	0.23 $m_e^*(\Gamma_1)$ $m_h^*(\Gamma_7)$			Crystallization form not known
Polytype (4H)	2.10 ± 0.10 ($\vec{E} \perp \vec{c}$)	0.17 ± 0.02				(0.015 ± 0.002) $\vec{F} \perp \vec{c}$, $\vec{E} \perp \vec{c}$
	2.10 ± 0.10 ($\vec{E} \parallel \vec{c}$)	0.19 ± 0.02				
Hexagonal (2H)	1.82 ± 0.10 ($\vec{E} \perp \vec{c}$)	0.22 ± 0.04	0.23 $m_e^*(\Gamma_7)$ $m_h^*(\Gamma_7)$	0.25 $m_e^*(\Gamma_7)$ $m_h^*(\Gamma_9)$	0.18 $m_e^*(\Gamma_7)$ $m_h^*(\Gamma_9)$	(0.023 ± 0.003) $\vec{F} \perp \vec{c}$, $\vec{E} \parallel \vec{c}$
	1.78 ± 0.10 ($\vec{E} \parallel \vec{c}$)	0.26 ± 0.04	0.27 $m_e^*(\Gamma_7)$ $m_h^*(\Gamma_7)$	0.32 $m_e^*(\Gamma_7)$ $m_h^*(\Gamma_9)$	0.23 $m_e^*(\Gamma_7)$ $m_h^*(\Gamma_9)$	(0.019 ± 0.002) $\vec{F} \parallel \vec{c}$, $\vec{E} \perp \vec{c}$ (0.025 ± 0.003) $\vec{F} \parallel \vec{c}$, $\vec{E} \parallel \vec{c}$

than expected by the results obtained by the $\vec{k} \cdot \vec{p}$ method.[19,20]

Previously,[1,2] a very small FKE was observed in 2*H* crystals. This was due to the almost inevitable presence of narrow stacking faults and their influence on the effective fields present in the hexagonal parts of the crystal. As the field was applied along the *c* axis, the fields were the largest around the stacking faults and very small in the homogeneous hexagonal part, as can be seen from the parallel case involving a cubic region illustrated in Fig. 3. The sandwich method made it possible to observe the real FKC in the hexagonal structure as reported here.

SUMMARY

Faulted ZnS crystals were studied with an uv scanning optical microscope. All measurements were carried out at room temperature. The results show that voltages applied parallel to the *c* axis give rise to highly inhomogeneous internal fields. These combine with the intrinsic electric fields which are due to the charged dislocation planes. The use of semitransparent evaporated electrodes which created fields perpendicular to the *c* axis made it possible to measure the true Franz-Keldysh coefficient and to compare the reduced effective masses in a number of crystals. Contrary to the previous measurements the use of this second method made it possible to show that the FKE in the hexagonal crystals is of the same order of magnitude as the effect in the cubic structure.

ACKNOWLEDGMENTS

The authors would like to thank to Professor I. T. Steinberger for frequent discussions, I. Natanson for growing the crystals, and the staff of the Department workshop for the construction of the microscope.

---

*Supported by the Central Research Fund of the Hebrew University.

[1]G. Shachar, Y. Brada, E. Alexander, and Y. Yacobi, J. Appl. Phys. 41, 723 (1970).
[2]Y. Brada, I. T. Steinberger, and B. Stone, Phys. Lett. A 38, 263 (1972).
[3]O. Brafman, E. Alexander, B. S. Fraenkel, Z. H. Kalman, and I. T. Steinberger, J. Appl. Phys. 35, 1855 (1964).
[4]I. T. Steinberger, E. Alexander, Y. Brada, Z. H. Kalman, I. Kiflawi, and S. Mardix, J. Cryst. Growth 13/14, 285 (1972).
[5]S. Mardix, Z. H. Kalman, and I. T. Steinberger, Acta Crystallogr. A 24, 464 (1968).
[6]S. Mardix and I. T. Steinberger, J. Appl. Phys. 41, 5339 (1970).
[7]G. Shachar and Y. Brada, J. Appl. Phys. 41, 3127 (1970).
[8]O. Brafman and I. T. Steinberger, Phys. Rev. 143, 501 (1966).
[9]W. Franz, Z. Naturforsch. A 13, 484 (1958).
[10]L. V. Keldysh, Zh. Eksp. Teor. Fiz. 34, 1138 (1958) [Sov. Phys.-JETP 7, 788 (1958)].
[11]G. Shachar, Ph. D. thesis (Hebrew University, 1969) (unpublished).
[12]J. Schanda, M. Somogyi, M. Gal, and G. Szigeti, J. Luminescence 1,2, 51 (1970).
[13]G. Shachar, Appl. Phys. Lett. 8, 282 (1966).
[14]O. Brafman, G. Shachar, and I. T. Steinberger, J. Appl. Phys. 36, 668 (1965).
[15]G. Shachar, Y. Brada, and I. T. Steinberger, J. Appl. Phys. 42, 872 (1971).
[16]J. C. Miklosz and R. G. Wheeler, Phys. Rev. 153, 913 (1967).
[17]M. Cardona, J. Phys. Chem. Solids 24, 1543 (1963).
[18]J. Schanda, J. Gergely, and M. Gal, Z. Naturforsch. A 24, 1353 (1969).
[19]G. Dresselhaus, A. F. Kip, and C. Kittel, Phys. Rev. 98, 368 (1955).
[20]E. O. Kane, J. Phys. Chem. Solids 1, 82 (1956).